Chapter IV. PROPOSED MEASUREMENT — OVERVIEW

This experiment is based on a technique to measure the neutron EDM, which is qualitatively different from the strategies adopted in previous measurements (see Chapter III). Chapter IV provides an overview of the general strategy, however, many crucial technical details that are essential to the success of the measurement are deferred until Chapter V.

The overall strategy adopted here[1a], is to form a three component fluid of neutrons and ^{3}He atoms dissolved in a bath of superfluid ^{4}He at ~300 mK. When placed in an external magnetic field, both the neutron and ^{3}He magnetic dipoles can be made to precess in the plane perpendicular to the B field. The measurement of the neutron electric dipole moment comes from a precision measurement of the difference in the precession frequencies of the neutrons and the ^{3}He atoms, as modified when a strong electric field (parallel) to B is turned on (or reversed). In this comparison measurement, the neutral ^{3}He atom is assumed to have a negligible electric dipole moment, as expected for atoms of low atomic number [1a].

A.   General Features

1.   Frequency Measurement

As discussed in Chapter III, over the forty-year history of experimental searches for the neutron EDM, d_n , a number of different techniques have been employed. However, in the last two decades the measurements have focused on the use of UCN constrained to neutron traps. The primary method is to study the precession frequency of neutrons with aligned spins in the plane perpendicular to a static magnetic field, B_0 . Application of a static electric field, E_0, parallel (anti-parallel) to B_0 can change the Larmor precession frequency, v_n , in proportion to the neutron EDM, d_n . The precession frequency is:

$$v_n = -[2\mu_n B_0 \pm 2d_n E_0]/h \equiv v_0 \pm (\Delta v/2) \qquad (IV.1)$$

where the minus sign reflects the fact that $\mu_n < 0$.

Thus the frequency shift, Δv , as the direction of E_0 is reversed, is:

$$\Delta v = -4d_n E_0/h \ , \qquad (IV.2)$$

In the case of $B_0 = 1$ mG and $E_0 = 0$, the Larmor precession frequency is $v_0 = 2.92$Hz. With $E_0 = 50$ kV/cm, and using a nominal value of $d_n = 4 \times 10^{-27}\, e$ cm, the frequency shift, as the electric field is reversed, is:

$$\Delta v = 0.19 \mu \text{Hz} = 0.66 \times 10^{-7} v_0 \ . \qquad \text{(IV.3)}$$

Note that for the current measurement, it is the absolute frequency shift, Δv, that is critical, not the fractional frequency shift. For a known electric field, E_0, the uncertainty in d_n is:

$$\delta d_n = h \frac{\delta \Delta v}{4 E_o} \qquad \text{(IV.4)}$$

2. *Statistical and Systematic Errors*

The immediate challenge of an EDM measurement of Δv is to generate as large an electric field as possible in the presence of a weak B field, and to measure a precession frequency shift with an absolute uncertainty $\delta \Delta v$ at the sub μHz level. Other issues include production of a large neutron sample size as well as having a precise knowledge of the spatial and temporal properties of B_0 and E_0.

Consider a measurement sequence in which N_0 neutrons are collected in a trap over a time T_0, followed by a precession measurement for a time T_m. This measurement cycle can be repeated *m* times for a total measurement time: $t = m\, T_m$. A single cycle takes a time: $T_o + T_m$ and the time to perform m cycles is: $m\, (T_o + T_m)$.

From the uncertainty principle we have

$$\delta \Delta v \geq \frac{1}{2\pi T_m \sqrt{N}} \qquad \qquad \text{per cycle}$$

The statistical contribution to the uncertainty in the EDM for the set of *m* measurements is:

$$\sigma \geq \frac{\hbar/4}{E_0 T_m \sqrt{Nm}} = \frac{\hbar/4}{E_0 \sqrt{T_m Nt}} \text{ecm} \ . \qquad \text{(IV.5)}$$

Here $N < N_o$ is the effective number of neutrons contributing to or detected in the measurement. Equation IV.5 is useful since it gives a lower bound on the statistical error. In practice it only gives an order of magnitude estimate for the statistical error of a generic experiment due to the ambiguity in the value of N. For the experiment discussed here, we do the proper analysis of the statistical error in Section V.H.

Consider the parameters typical of this proposed LANSCE measurement as discussed below: $E_0 = 50$ kV/cm, $T_O = 1000$ sec, $T_m = 500$ sec, $N = 4.0 \times 10^6$ neutrons / measurement cycle and $m = 5.7 \times 10^3$ repeated cycles (1500 sec / cycle and 100 days of live time). Three other parameters, also discussed below, characterize the three neutron loss mechanisms:

Beta decay: $\tau_\beta = 887$sec, wall losses $\tau_{wall} = 1200$sec,
and n - ^{3}He absorption $\tau_3 = 500$sec

Using Eq. (IV.5) with the overestimate, $N = N_O$, gives for one standard deviation uncertainty: $\sigma \geq 10^{-28}$ e cm. See however, the more realistic calculation (including shot noise) given in Section V.H, which gives a 2σ limit of 9 x 10^{-28} e cm.

One can compare this result to the error on the 1990 Smith [1], ILL measurement where they achieved:

$$d_n = -3 \pm 5 \times 10^{-26} \ e \ \text{cm}.$$

where the error is from both statistical and systematic contributions. For the more recent Harris [2], ILL measurement they achieve:

$$d_n = -1 \pm 3.6 \ \text{x} \ 10^{-26} \ e \ \text{cm}.$$

For statistical errors, note that the quality factor, $E_0 \sqrt{(T_m N)}$ in Eq. (IV.5), gives a relative reduction in σ by a factor of 50 to 100 at LANSCE, in comparison to the Smith [1] ILL measurement and to the Harris [2] ILL measurement.

The challenges in designing this trapped UCN experiment were to maximize N_0, T_m, and E_0. In addition it is crucial to develop uniform, stable, and well measured B_0 and E_0 fields over the sample volume since these are a major source of systematic errors. The method developed to measure the errors related to B_0 are discussed below. More generally, issues related to systematic errors, such as v x E effects, pseudo-magnetic fields, gravitational effects, spatial differences in UCN/ ^{3}He distributions, etc., are discussed in detail in Section V.H.

In the technique adopted here, there are three critical issues that are addressed in this overview:

1. Optimize the UCN trap design for large N_O, long trap lifetime, and large E_0.

2. Make a precision measurement of the B_O field, averaged over the neutron trap volume and valid for the neutron precession period.

3. Make a precision measurement of the neutron precession frequency, ν_n.

The overall layout of the experimental apparatus is shown in Fig. IV.1

B. Neutron Trap Design

We use the strategy for loading the trap with UCN suggested first by Golub [3]. It relies on using UCN locally produced inside a closed neutron trap filled with ultra-pure, super-fluid ^{4}He, cooled to about 300 mK When this neutron trap is placed in a beam of cold neutrons (E = 1 meV, v = 440 m/s, λ = 8.9 Å, see section V.A) the neutrons interacting with the superfluid may be down-scattered to $E < 0.13~\mu$ eV, v < 5 m/s with a recoil phonon in the superfluid carrying away the missing energy and momentum.

The properly averaged UCN trapping (production) rate [4], as discussed in Section V.B, gives a nominal trapped UCN production rate, P, of
$$P ~\sim~ 1.0 \text{ UCN/ cm}^3 \text{ sec}$$
In order to minimize neutron absorption by hydrogen, deuterated polystyrene coatings have been developed for the surfaces of the trap (see discussions in [5]). The goal for the mean life of a neutron in a trap filled with pure ^{4}He and operated at 300 mK is about 500 sec as a result of losses by neutron beta decay and neutron wall interactions.

In T_0 = 1000 sec of UCN production, the neutron density will reach $\rho_n \sim 500$ UCN/cm^3 in the ^{4}He. Note that at other facilities with more intense sources of cold neutrons this density could be considerably higher. This UCN production technique and the UCN production rate calculations for a ^{4}He filled UCN trap have been tested and validated by Golub [3], and at the neutron lifetime experiment now in progress at NIST [6] (see Section V.B).

The details of the proposed geometry for the target region of the experiment are shown in Figs. IV.1 and IV.2, with two trap volumes, one on each side of the high-voltage central electrode. Thus two orientations of the electric field for a fixed B field will be measured simultaneously. Superfluid ^{4}He is a very good medium for high electric fields (see [7] and section V.E) and experience has shown that the deuterated polystyrene surfaces are very stable under high E fields [5]. Independent bench tests are planned in order to

evaluate the trap performance under these conditions. The goal is to operate at an E field strength of 50 kV/cm (about four times greater than other recent EDM measurements).
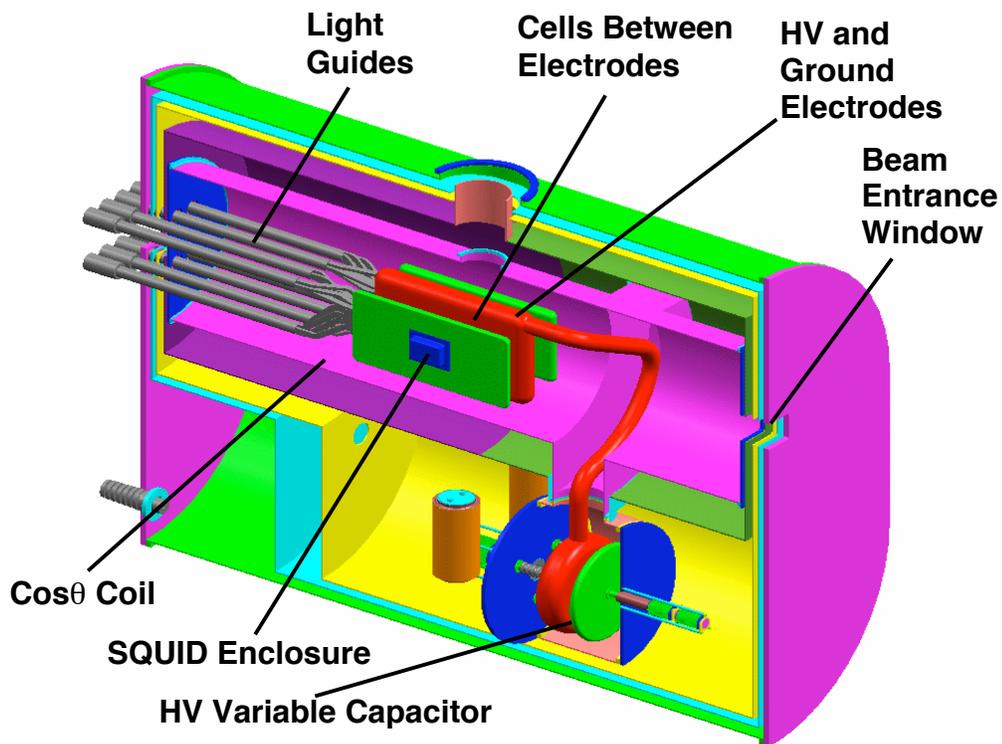

Fig IV-1. Experimental cryostat, length ~ 3.1 m. The neutron beam enters from the right. Two neutron cells are between the three electrodes. Scintillation light from the cells is monitored by the light guides and photomultipliers.

Properties of the magnetic and electric fields are discussed in Section V.E. The region in the cryostat but outside the UCN cells (see Fig. IV-1) will also be filled with ^{4}He because of its good electrical insulating properties. Note: The ^{4}He fluid in the region outside the two UCN cell volumes will contain ^{3}He atoms at normal concentrations (see below). Any UCN produced there will be absorbed in coatings on the vessel wall to prevent wall activation.

C. Measurement of the B Field with a ^{3}He Co-Magnetometer

Knowledge of the B field environment of the trapped neutrons is a crucial issue in the analysis of systematic errors in the measurement. The ^{4}He-UCN cells will sit in the uniform B field of a Cos Θ magnet with a nominal strength of 1 mG (up to 10 mG). The B field must be uniform to 1 part in 1000 (see Section V.E). These features of the B field must be confirmed by direct measurement in real time.

The magnetic dipole moment of ^{3}He atoms is comparable to that of the neutron (see Table I-B) such that the ^{3}He magnetic dipole moment is only 11% larger than that of the neutron. In addition, the EDM of the ^{3}He atom is negligible due to the shielding from the two bound electrons [1a] i.e. Schiff shielding [8]. These properties make ^{3}He an excellent candidate as a monitor of the B field in the volume where the UCN are trapped, or if B is stable, as a reference for precession frequency measurements.

To exploit this, the pure ^{4}He superfluid is modified by adding a small admixture of polarized ^{3}He (with spins initially aligned with the B_O field). The amount is ≈ 1 x 10^{+12} atoms / cm^3 and fractional density of $X = 0.4$ x 10^{-10}. This mixture is prepared in a separate reservoir and then transferred to the neutron cells. The result is a three-component fluid in the cell with densities: $\rho_n = 5.0$ x 10^{+2}/ cc, $\rho_3 = 0.8$ x 10^{+12}/ cc, and $\rho_4 = 2.2$ x 10^{+22}/ cc.

The UCN cells will be adjacent to SQUID coils mounted in the ground electrodes as discussed in Section V.F and V.H. The spins of the ensembles of ^{3}He and neutrons are aligned (see below) and are initially parallel to the B_0 field. An "RF coil", positioned with its axis perpendicular to B_0 (see Section V.E), is then used to rotate the neutron and ^{3}He spins into the plane perpendicular to B_0. We discuss the resulting n-^{3}He interaction below.

As the spins of the ^{3}He atoms and the neutrons precess in this plane, the SQUID coils will pick up the signal from the large number of precessing ^{3}He magnetic dipoles; the corresponding neutron signal from 500 UCN/cm^3 is negligible. Analysis of this
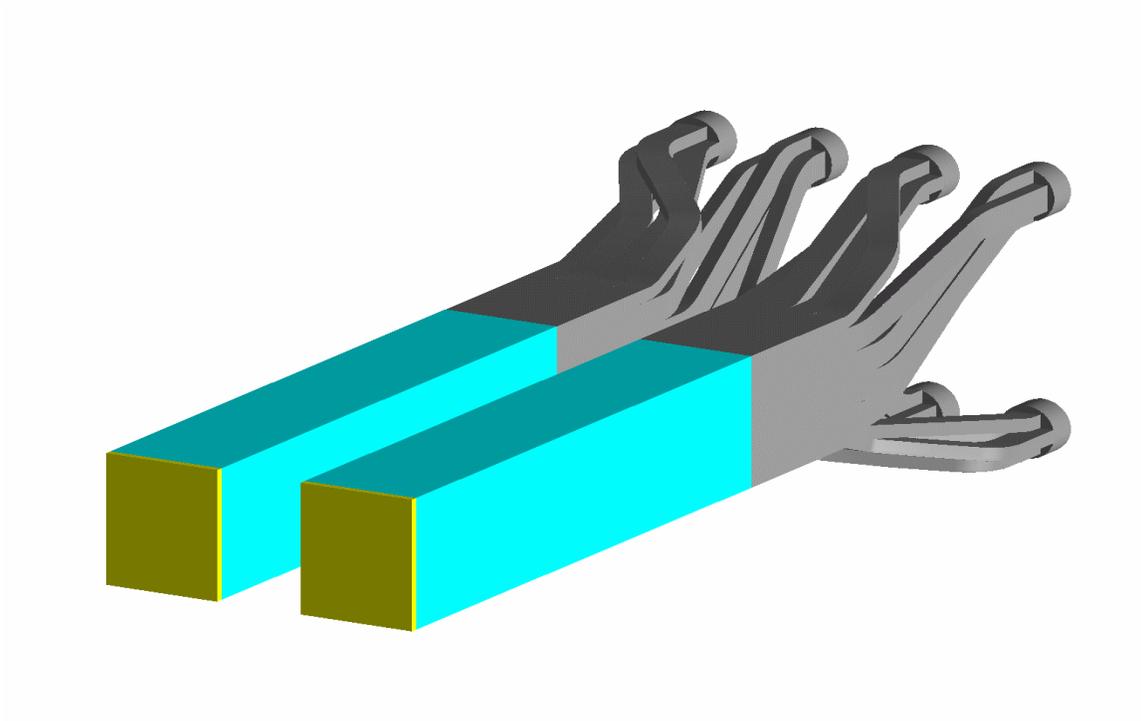
Fig IV-2. Two cell design with light guides which connect to the photomultiplier tubes outside the cryostat. Each cell has a nominal volume of 4 L.

sinusoidal signal will directly measure the ^{3}He precession frequency, ν_{3}, and thus the magnetic field, B_{0}, averaged over the same volume and time interval as experienced by the trapped UCN's.

$$B_{0} = -\frac{\nu_{3}}{2\mu_{3}} \ . \tag{IV.6}$$

In summary, the addition of the ^{3}He atoms to the measurement cells and the SQUIDs to the electrodes, provides the opportunity for a direct measurement *in situ* of the B field averaged over the cell volumes and the time period of the measurement.

D.   Measurement of the UCN Precession Frequency

Knowledge of the neutron EDM depends on a precision measurement of the change in the neutron precession frequency for the two orientations of the electric field. Consider N_{0} UCN trapped in a cell. Because the magnitude of the precession frequency shift, $\Delta\nu_{n}$, due to the interaction of the neutron EDM with the electric field, is extremely small,

<1 μ Hz, it is imperative to measure it with great precision. The technique adopted here is to make a comparison measurement in which ν_n is compared to the ^{3}He precession frequency, ν_3. The technique relies on the spin dependence of the nuclear absorption cross section for the reaction:

$$n + {}^3\text{He} \rightarrow p + t + 764 \ \text{keV}. \tag{IV.7}$$
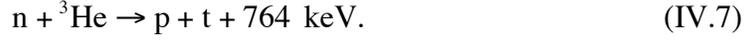
The nuclear absorption reaction products (and the neutron beta decay products) generate scintillation light in the ^{4}He fluid, which can be shifted in wavelength and detected with photomultipliers.

The absorption cross section is strongly dependent on the initial spin state of the reaction:

Spin State	Cross Section, σ_{abs}, barns [10]	
	(v = 2200 m/sec)	(v = 5 m/sec)
$J = 0$	~ 2 x $5.5 \times 10^{+3}$	~ 2 x $2.4 \times 10^{+6}$
$J = 1$	~ 0	~ 0

There are two options here. In **option A**, where the cell is irradiated with an unpolarized cold neutron beam, we take $\sigma_{abs} = 2.4 \times 10^6$ b as the average ^{3}He absorption cross section for UCNs. The mean life of the neutron in the trap due to ^{3}He absorption alone, τ_3, is given by:

$$1/\tau_3 = \rho_3 \left[\sigma_{abs} v \right]_{UCN} = \rho_3 \left[\sigma_{abs} v \right]_{thermal} . \tag{IV.8}$$

The ^{3}He density, ρ_3, is adjusted to give $\tau_3 = 500$ sec. This corresponds to:

$$\rho_3 = 0.85 \times 10^{+12} \ {}^3\text{He} / \text{cm}^3.$$

The net neutron mean life in the trap is 250 sec, due about equally to losses by ^{3}He absorption and by neutron beta decay/ wall losses.

In this scheme, the only neutrons which survive are those with spins parallel to the polarization vector of the ^{3}He (and aligned with the B_o field). In the process, half the neutrons in the trap have been lost. We are assuming here 100% ^{3}He polarization and that there is no polarization loss in the traps.

An alternative approach, **option B**, is to pre-select the cold neutron beam according to spin direction, with an upstream spin selector, and to direct neutrons of each of the two transverse spin orientations to each of the two cells. Although there may be flux losses in the spin selector apparatus, the subsequent loss of neutrons to ^{3}He absorption in a cell will only occur if there is not perfect ^{3}He or neutron-beam polarization or if there is loss of polarization in the cell as time passes. Over all this approach makes the measurement less sensitive to the ^{3}He polarization in the cells (see Section V.D).

As noted, there are three neutron loss mechanisms in the cells which lead to: $\tau_\beta = 887$ sec, $\tau_3 = 500$ sec, $\tau_{cell} \sim 1200$ sec. During the precession process in the cell, as a result of all three loss mechanisms, the net neutron mean life is: $1/\Gamma_{avg} = 250$ sec. On the other hand, during the UCN production phase in which a cold polarized beam of neutrons is aligned with the polarized ^{3}He in the cell, there are no absorption losses and the mean neutron life in the cell is 500 sec. Effects due to time dependent polarization changes in the cell are neglected in this discussion (section V.C and V.H). This second strategy, **option B**, is being evaluated and is discussed in Section V.A.

To start the precession process, independent RF coils are used to reorient the neutron and the ^{3}He spin directions into the plane perpendicular to B_0 where they both precess about B_0, initially with their spins parallel. Thus the aligned ^{3}He and UCN components are trapped in the cell and continue to precess for up to a time, T_m, at which point the cell is flushed so a new measurement cycle can begin.

However, because the magnetic dipole moments of the neutron and ^{3}He are slightly different :

$$\mu_{^3He}/\mu_n = 1.11 \ ,$$

the ^{3}He spin vectors will gradually rotate ahead of the neutron spin vectors and destroy the alignment. As the precession continues, the absorption process will alternately appear and disappear.

This absorption process can be observed as scintillation light generated by the recoiling charged particle reaction products in the ^{4}He superfluid. The scintillation light is emitted in a broad spectrum centered at 80 nm, and is easily transmitted to the wall of the cell where a deuterated tetraphenyl butadiene-doped polystyrene surface will absorb it and re-emit it at 430 nm. This wave-shifted light can be collected with light pipes and transmitted to photomultiplier tubes outside of the B field region (see Section V.C).

The net scintillation light signal, $\Phi(t)$, due to a constant background, Φ_{bgd}, beta decay, and ^{3}He absorption, and with polarizations P_3 and P_n, can be written as (see V.H):

$$\Phi(t){=}\Phi_{bgd}{+}N_o\exp(-\Gamma_{avg}t)\left\{\frac{1}{\tau\beta}+\frac{1}{\tau3}\left(1-P_3P_n\cos\left[(\nu_3-\nu_n)t+\phi\right]\right)\right\}$$

Equation IV.9

where we neglect the loss of both neutron and ^{3}He polarization during the measurement period. Here Γ_{avg} is the overall neutron loss rate for the cell including both wall losses and neutron beta decay as well as absorption. The neutron scintillation rate has a time dependence coming from both the decaying exponential factor and the sinusoidal dependence on: $\nu_3 - \nu_n = 0.3$ Hz.

The resulting photomultiplier signal gives a direct measure of the neutron precession rate, ν_n, when combined with a knowledge of ν_3.

In summary, the introduction of $0.8 \times 10^{+12}$ polarized ^{3}He atoms/cm^3 into a cell containing $5 \times 10^{+2}$ UCN/ cc allows one to directly measure the average B_O field and to confirm the polarization of the UCN. It also permits a direct and precise measurement of the orientation of the UCN spin relative to the ^{3}He spin as they precess over a time interval, $T_m = 500$ sec (two neutron mean cell life times). It is this time-dependent absorption sinusoidal light signal which must be carefully analyzed for changes in its period as the E_0 field is reversed.

For this two component fluid of neutrons and ^{3}He dissolved in the ^{4}He super-fluid we measure:

$$\nu_3 =-2\mu_3B_0 \ , \tag{IV.10}$$

obtained from the SQUID signal, and

$$\nu_n = -\left[2\mu_nB_0 + 2E_0d_n\right]/h \ , \tag{IV.11}$$

obtained from the combination of the scintillation light and the SQUID signals. Thus analysis of the shape and the time dependence of the scintillation light signal, throughout the precession period, is critical to the precision of the EDM measurement.

Note that when $E_O = 0$, the two measurements (SQUID and scintillation signals) can be crossed checked since they should both give the common value of B_O. Alternatively, for a stable B_O field and when $E_O \neq 0$, the SQUID measurement provides a reference clock against which a shift in the scintillator spectrum can be measured.

E.   Discussion of Errors

The most vexing problem in the design of a neutron EDM measurement is the control of systematic errors. This is amply illustrated by the discussion of previous neutron EDM measurements reviewed in Chapter III. This overview addresses only a few aspects of the problem; the details are deferred to the main discussion in Section V.H.

1.   Statistical Errors

The gross analysis of the statistical errors presented above, equation IV.5, suggests that the proposed technique gives an improvement in the figure of merit $E_0 \sqrt{(T_m N_o)}$ by a factor of 50 – 100 over recent UCN measurements at ILL. Subsidiary measurements planned for LANSCE, involving cell fabrication tests, cold neutron flux measurements, and maximum usable E field tests, will verify whether this gain can be fully realized.

2.   Systematic Errors

The analysis of systematic errors is a challenging and detailed exercise and is at the heart of a successful EDM measurement. The major concerns are related to knowledge of the magnetic and electric fields (since both time-dependent field strengths and nonparallel E and B fields, have the potential to produce a false EDM signal), any differences in the two cells, and any contribution of background sources to the scintillation light spectrum.

The ^{3}He-precession measurement allows the magnetic field to be sampled in time and space throughout the precession period and over the volume of the UCN traps. The major limitations come from the quality, stability, and background of the SQUID signals. Bench tests of the performance of the SQUID coils at these low temperatures and in the LANSCE noise environment are in progress as discussed in Section V.F. The goal is a B_O field uniform to 0.1 % over the cell volume.

The electric field properties are equally critical. The goal for the electric field uniformity is < 1 % as discussed in Section V.E. In order to achieve the high fields consistent with the dielectric properties of the superfluid ^{4}He medium, a program for performing bench tests of the maximum useable electric field is being developed. Issues of leakage currents and sparks are critical and in the end will dictate the upper limit at which the applied voltage can operate.

Other issues, related to the properties of the cold neutron beam, pre-selection of the neutron spin, and the role of gamma-ray and neutron induced backgrounds, are discussed in Sections V.A and V.C. The optimum sequence in the measurement cycles in order to cancel systematic shifts in the data also has to be evaluated.

F. Measurement Cycle

By way of clarification and review, we describe the measurement sequence over the 1500 sec measurement cycle, as currently envisioned, with some additional details included.

1. **Cold neutron beam preparation.** Cold neutrons (v= 440 m/s, 1 meV) from the LANSCE liquid-hydrogen moderator, are transported by neutron guides through a frame overlap chopper, T_O chopper, and a Bi filter. This system (see Section V.A) filters out unusable neutrons and gamma rays. In addition the beam is divided into two guides that transport the cold neutrons downstream and through the cryostat wall to the two cells. We are currently evaluating techniques to install a spin filter in the guide (**option B** in the above discussion) to permit pre-selection of the neutron spin state. Spin rotators make both beams have their spins aligned with the ^{3}He atoms in the measuring cells. The technology to divide the beam is available, but the cost in loss of flux and beam line floor space is still being evaluated. The splitter is discussed in Section V.A and Appendix A.

    For the purposes of this discussion of the measurement cycle, we assume that the beam is split into two components matched to the neutron cell sizes and that the beam spin filter is implemented. We further assume that E_O and B_O are on and stable during the entire cycle.

2. **^{4}He and polarized ^{3}He transfer to the cells.** – START OF A 5-STEP CYCLE. During a previous measurement phase (step 5 below), polarized ^{3}He (~99% polarization and density fraction X ~ 10^{-10}) from an atomic beam apparatus, is mixed with ultra-pure superfluid ^{4}He in a reservoir separate from the target cells. Now, with the beam shutter closed, the mixture is transferred to the measurement cells. A small holding field continues to be used to maintain the polarization during the transfer, < 10 sec. The ^{3}He polarization is selected in the polarized source to be either parallel or anti-parallel to the magnetic field, Bo, generated by the cos Θ magnet. The ^{3}He spin vectors are the same in both cells, but, by construction, the electric

fields are opposite of each other, regardless of the sign of the potential on the high-voltage electrode.

3. **Cold neutron beam irradiation and production of the UCN in the cells.** The beam shutter is opened, allowing the cold neutrons to irradiate the cells, some of which produce UCN. The two cells, each filled with superfluid ^{4}He (2.2 x 10^{22}/cm^3) and polarized ^{3}He (0.8 x 10^{+12} /cm^3), are irradiated for $T_O = 1000$ sec. A trapped sample of UCN is built up with a production rate of $P = \sim 1$ UCN / (cm^3 sec). The mean life of these neutrons in the cells is ~ 500 sec due to both beta decay and wall losses alone. Assuming that the initial sample of neutrons has been fully polarized, the large n-^{3}He cross section in the $J = 0$ state will reduce only slightly the population of neutrons during the UCN collection process. Neutrons properly aligned with the ^{3}He will suffer no absorption losses. The number density produced in $T_O = 1000$ sec grows to $\rho_n \sim 500$ UCN/ cm^3 (actually 430/ cm^3 when corrected for beta decay and cell losses) in each of two cells of volume = 4000 cm^3 per cell. At the end of the UCN fill period, the beam shutter is closed.

4. **Rotation of both magnetic moments into the transverse plane.** The spin vectors are rotated into the plane perpendicular to B_O and E_O by pulsing an "RF" coil at 3.165 Hz for 1.58 sec (see Section V. E). Both the neutrons and the ^{3}He start to precess about B_O in order to conserve angular momentum.

5. **Precession Frequency measurements.** The critical precession frequency measurement occurs over the next $T_m = 500$ seconds. At the start of the measurement there are 4 x 10^{+6} neutrons in the two traps. The SQUID detectors measure the ^{3}He precession, ν_3, at about 3 Hz over a set of 1500 signal periods. The scintillator detection system measures $\nu_3 - \nu_n = 0.3$ Hz over a set of 150 signal periods. The neutron sample continues to decrease with a mean life of 250 sec due to all loss mechanisms and is reduced to 116 UCN/cm^3, i.e. a total of 0.5 x 10^{+6} neutrons at the end of the measurement cycle. As discussed in detail in Section V.H, this corresponds to a sensitivity of
$$\sigma \sim 7 \text{ x } 10^{-26} \text{ e cm in one cycle.}$$
In parallel with the precession measurement, the mixing reservoir is refilled with pure ^{4}He and polarized ^{3}He in the correct proportions.

6. **Empty the cells.** Valves are opened to drain the cells in about 10 sec, and the ^{3}He-^{4}He mixture is sent to a recovery reservoir for purification.
END OF THE CYCLE, return to step #2.

7. **Repeated cycles.** A single cycle takes about To + T_m = 1500 sec plus some transfer times. The cycle can be repeated about m = 5.7 x 10^3 time in 100 days, which gives a two σ limit of < 9 x 10^{-28} e cm in one hundred days.

Over this 100-day period one expects to follow a program of electric field reversals, spin reversals, magnetic field reversals, etc. to study and remove systematic effects.

Altogether this measurement involves the interplay of many technical and practical issues: polarized UCN and ^{3}He production, precision measurements of frequencies, UCN trap design, electric and magnetic field measurements, etc. These issues are discussed in detail in the following segment, Chapter V.

References

[1a] I B. Khriplovich, S.K. Lamoreaux, "CP Violation Without Strangeness", Springer-Verlag, (1997).

[1] K. F. Smith et al., *Phys. Lett.* **234B**, 191 (1990).

[2] P. G. Harris et al, *Phys. Rev. Lett.* **82**, 904 (1999).

[3] P. Ageron et al, Phys Lett. **A66**, 469 (1978), R. Golub et al, *Z. Phys.***B51**, 187 (1983), R. Golub, *J. Phys.* **44**, L321 (1983); Proc. 18th Int. Conf. on Low Temperature Physics, Pt. 3 Invited Papers (Kyoto, Japan), 2073 (1987), R. Golub and S. Lamoreaux, *Phy. Rep.* **237**, 1 (1994).

[4] S. K. Lamoreaux and R. Golub, *JETP Lett.* **58**, 793 (1993).

[5] S. K. Lamoreaux, Institut Laue-Langevin Internal Report 88LAOIT, 1988, unpublished; J.M. Pendlebury, *Nuc. Phys.* **A546**, 359 (1992).

[6] P. R. Hoffman et al., *Nature* **403**, 62 (2000).

[7] J. Gerhold, *Cryogenics* **12**, 370 (1972).

[8] L. I. Schiff, *Phys. Rev.* **132**, 2194 (1963); Quantum Mechanics, third edition (New York: McGraw-Hill, 1968).

[9] Superfluid He is a well known scintillator for:
electrons: M. Stockton et al., *Phys. Rev. Lett.* **24**, 654 (1970).
alpha particles: H. A. Roberts and F. L. Hereford, *Phys. Rev.* **A7**, 284 (1973). D. N. McKinsey et al, *NIM* **B132**, 351 (1997), D. N. McKinsey et al, *Phys. Rev.* **A59**, 200 (1999).